Energy 173 (2019) 38–47

Contents lists available at ScienceDirect

Energy

journal homepage: www.elsevier.com/locate/energy

Energy saving with Optic-Variable Wall for stable air temperature control

Cheng Wang [a, *], Xiaofeng Guo [b, c], Ye Zhu [d, **]

[a] Jiangsu Provincial Key Laboratory of Oil & Gas Storage and Transportation Technology, Changzhou University, Changzhou, 213016, Jiangsu, PR China
[b] University of Paris Diderot, Sorbonne Paris Cité, LIED, UMR 8236, CNRS, F-75013, Paris, France
[c] ESIEE Paris, University of Paris Est, 2 Boulevard Blaise Pascal - Cité Descartes, F-93162, Noisy Le Grand, France
[d] Jiangsu Provincial Key Laboratory of Fine Petrochemical Engineering, Changzhou University, Changzhou, 213164, Jiangsu, PR China

ARTICLE INFO

Article history:
Received 20 October 2018
Received in revised form
16 January 2019
Accepted 6 February 2019
Available online 7 February 2019

Keywords:
Optic-variable wall (OVW)
Optic-fixed wall (OFW)
Energy saving
Heating & cooling
Stable air temperature control

ABSTRACT

Optic-Variable Wall (OVW) holds the property of tunable reflectivity to solar radiation. By allowing more solar radiation absorption in winter while maintaining high reflection in summer, OVW can help energy-saving during the HVAC of buildings. In this paper, the energy saving potential with OVW for stable air temperature control is investigated. Annual meteorological conditions are adopted in the comparison of cooling and heating loads. The effects of properties of OVW and Indoor Air Temperature (IAT) are discussed. It is concluded that OVW is able to simultaneously reduce heating and cooling loads. The optimum onset temperature of OVW is half the temperature zone lower than IAT. With the adoption of OVW, the heating load is close to the case of OFW (Optic-Fixed Wall) with low reflectivity; the cooling load of OVW provides close effect as using high-reflectivity OFW. In terms of tuning temperature, narrow temperature zone is favorable for the reduction of HVAC load. Comparing with OFW, the relative reduction of HVAC load with OVW is independent of conductive thermal resistance, corresponding to the thickness of insulation layer. The results offer new choices for the passive design of green buildings and show directions for future development and performance improvement of OVW.

1. Introduction

Heating, Ventilation and Air-Conditioning (HVAC) in the building sector represents a large portion of energy consumption in society [1]. To achieve the goal of energy saving and sustainable development, besides the performance improvement of active HVAC devices or systems [2–7], considerable passive measures are taken to the building itself [8–16]. These measures include passive heating in cold seasons [10,11], natural ventilation in hot seasons [12,13], reinforced thermal insulation [14,15] as well as peak shifting by heavy thermal mass [16]. While the above techniques act mostly on heat diffusion in the building envelop and the convective heat exchange between the building and ambience, some emerging technologies are developed to modulate the radiative heat transfer. These technologies mainly include radiation cooling [17–19] and the adjustment of solar radiation absorption (or reflection) [20–25].

Concerning energy consumption, HVAC load is usually traced back to two elements: outdoor ambient condition and occupant's behavior. In the case of stable indoor air temperature control, the occupant's demand is considered rigid, conforming to the design of processing parameters or indoor thermal comfort. Regarding the ambient condition, the key parameters are the ambient temperature and solar irradiance. Besides these two main factors, the wind speed and the surrounding constructions, etc., also have secondary influence on the heating or cooling load of buildings. The adoption of *passive* technologies is mainly aimed to reduce the HVAC load dependent to the difference between the ambient condition and the comfortable indoor temperature zone [26].

In most building structures, the opaque part, i.e. the wall, is the largest contact intermediate between the indoor air and ambient conditions. Windows, even double-layer ones, often results in higher HVAC loads due to the solar penetration into the indoor area. Architects are constantly facing the dilemma of either letting more daylight natural lighting in through large windows or meeting high energy-saving standards. In this sense, the effective energy saving

* Corresponding author.
** Corresponding author.
E-mail addresses: wangcheng3756@163.com (C. Wang), zhuy.6842@163.com (Y. Zhu).

https://doi.org/10.1016/j.energy.2019.02.051
0360-5442/

by opaque structure allows the design of larger area of transparent structure, such as window or glass curtain. Therefore, the wall structure with energy-saving property arouses increasing attention from many researchers [27–29], including this paper.

When the opaque wall is taken into consideration, the load for air-conditioning (cooling) and heating is modeled with the temperature difference between the outer wall and the indoor air, as well as the conductivity and the thickness of the wall/insulation layers. The smaller the temperature difference, the lower the heating or cooling load. When the indoor air temperature is maintained constant, the reduction of the temperature difference lies mostly on the adjustment of the outer wall temperature, e.g. towards warmer values in winter and cooler ones in summer. Due to the fact that the outer wall temperature is determined comprehensively by the solar radiation as well as the ambient temperature, the adjustment of solar radiation absorption or reflection will modify the wall temperature and ultimately adjust the HVAC load in buildings [30].

Several recent publications use the principle of adjustment on solar radiation absorption or reflection. Goldstein et al. [31] reported that the reflection of solar energy and emission at certain wavelength will generate cooling power in hot dry weather. Recently, a continuous kW-scale cooling test is reported [32]. However, radiative cooling is useful only in cooling dominated hot conditions and thus plays no role for heating reduction in winter. Zhu et al. [33] reported a long-time period experiment on a passive house with color-change in summer and in winter. The results show good performance in Dalian city, situated in the North of China. Zhang et al. [34] studied the performance of cooling energy saving by coating solar reflective material on building envelops. The average indoor air temperature is reported to be of 2.4 °C lower than the reference box without the above coating. More recently, Wang et al. [30] proposed Optic-Variable Wall (OVW) to automatically adjust the solar reflectivity in seasons, verified the feasibility with preliminary winter experiments and analyzed theoretically the performance on air temperature control in containers. However, in this reference, the energy-saving potential is proposed, while not quantitatively evaluated. The effects of OVW properties are not discussed in detail. Moreover, the indoor air temperature is not strictly kept constant.

In the current paper, the energy-saving potential of HVAC in buildings with OVW is theoretically analyzed in whole-year period with typical meteorological conditions of Shanghai city in China. The buildings are designed for stable indoor air temperature control, i.e., through HVAC. The ideal temperature responsive reflectivities of the OVW are taken as inputs. The effects of the properties of OVW, e.g. the onset temperature of OVW and the temperature zone of optic-variation, and the arbitrary air temperature inside, on the HVAC energy-saving potential are discussed. The results offer new choices for the design of green buildings and the reduction of HVAC load, and give useful guidance for the performance improvement in future studies.

2. Physical model

An OVW is able to automatically adjust its absorptivity, according to the temperature variation. The samples of lab developed OVW are shown in Fig. 1. Our previous experiments found that OVW is dark at low temperature and light at high temperature. The onset temperature and the temperature zone of optic-variation are respectively 33 °C and 3 °C, meaning a high reflectivity at above 36 °C and low reflectivity at below 33 °C. The reflectivity, measured with Shimadzu 3600 UV–Vis–NIR, is estimated as 0.15 at low temperature and 0.45 at high temperature. With the principle of optic-variation, the onset temperature of OVW as well as the temperature zone of optic-variation can be modulated, and the ideal reflectivity of OVW is expected to be 0.1 at low temperature to 0.9 at high temperature.

When OVW is adopted, the surrounding of buildings may include the roofs with different slopes, the walls with different orientations as well as the floor contacting with the environment different from the ambient conditions. For simplification concerns, in this paper, we adopted a multi-layer heat transfer model depicted in Fig. 2. The simplified model is composed of three main parts: (1) the ambient conditioned with ambient temperature T_{ao} and solar irradiance I, (2) the opaque wall characterized with conductive thermal resistance R_w and reflectivity ρ and (3) the indoor conditioned with indoor temperature T_{ai}. The background radiation, the reflective radiation as well as the convective heat transfer between outside of the wall and the ambient are integrated into the ambient comprehensive heat transfer coefficient h_o.

The ambient condition is cited from meteorological data and the stable indoor air temperature is prescribed at 25 °C. Since the indoor condition is kept constant, the heat flux Q through the wall is determined, which is then considered as the HVAC load of the buildings.

When the orientation of wall, neither horizontal nor vertical, should be considered, for instance, in the case of sloped roof, it is easy to take into consideration of the modification of solar radiation. When the surrounding condition of the building should be considered, e.g. in the wild field or surrounded by other buildings, it is easy to take the consideration of these factors into the

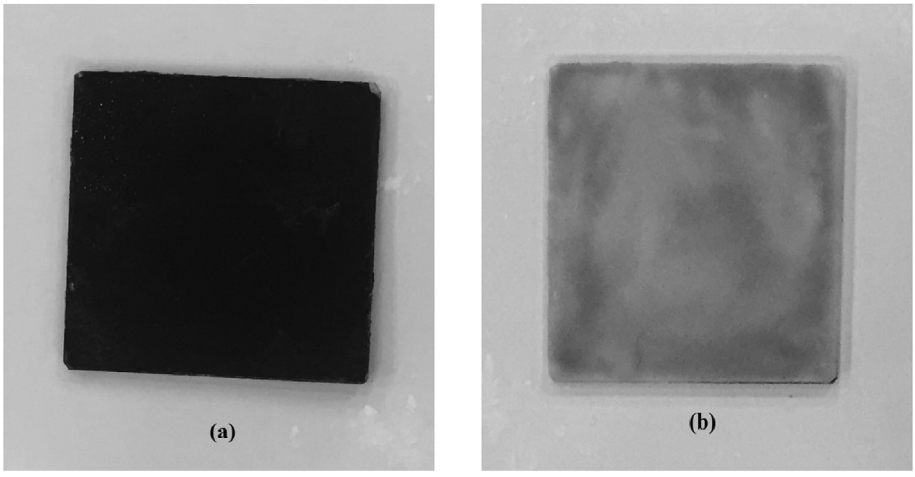

Fig. 1. Sample color-test of OVW. (a) Low temperature at 20 °C and (b) High temperature at 45 °C (Note: the non-uniform color distribution of OVW at high temperature is due to inhomogeneous temperature control limited by test conditions.).

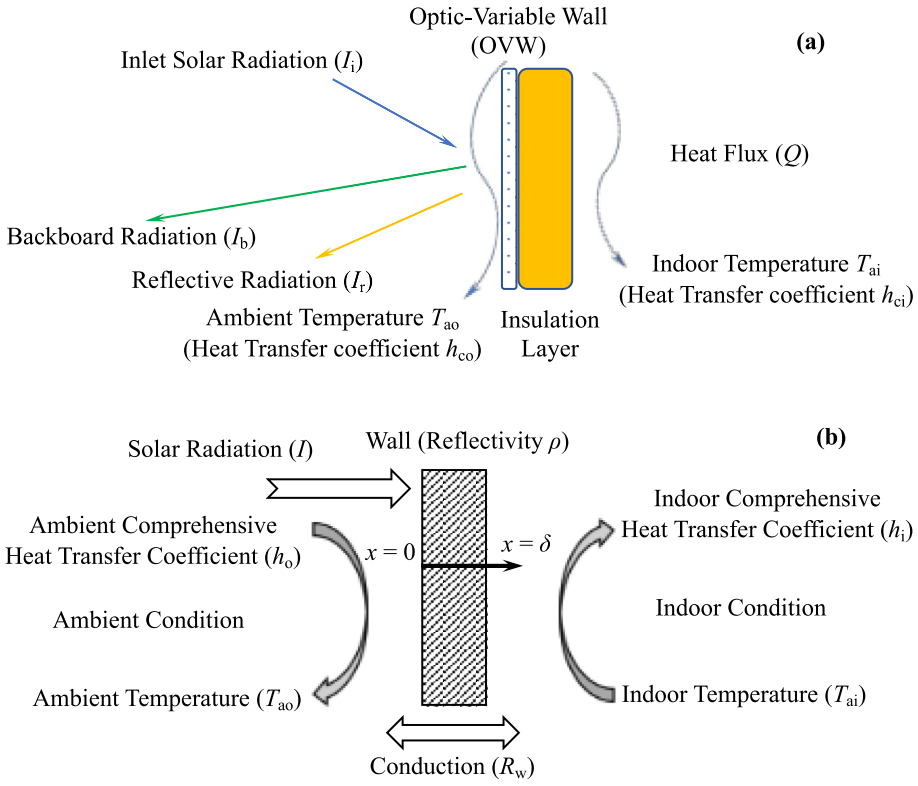

Fig. 2. Model of buildings with OVW. (a) Physical Model and (b) Simplified Model.

modification of comprehensive coefficient between the ambient and the wall. The properties of insulation layer, such as the thickness or the thermal conductivity, are integrated into the conductive thermal resistance R_w. The wall is considered as light-mass for structure weight limitation or convenient mobility, if necessary.

3. Determination of HVAC load

As mentioned above, HVAC load can be considered equal to the heat flux Q, as far as the indoor condition is prescribed and no other heat loads is considered. When the heat flux Q flows from the ambient to the indoor space, it is named as the cooling load and assigned positive. When the heat flux Q flows in the reverse direction, it is named as the heating load and assigned negative.

Since the time interval of meteorological data is 1 h, the heat transfer process can be treated as quasi-stationary. Therefore, the heat flux Q is expressed as:

$$Q = (1-\rho)\cdot I - h_o\cdot(T_{wo} - T_{ao}) \tag{1a}$$

where T_{wo} and T_{ao} refer to the temperature of outside wall and ambient air, respectively, I represents the solar irradiance, h_o corresponds to the ambient comprehensive heat transfer coefficient, and ρ is corresponding to the reflectivity of OVW to the solar irradiance, which is expressed as:

$$\rho = \begin{cases} \rho_1 & (T_{wo} \le T_{s1}) \\ \rho_1 + \dfrac{T - T_{s1}}{T_{s2} - T_{s1}}\cdot(\rho_2 - \rho_1) & (T_{s1} \le T_{wo} \le T_{s2}) \\ \rho_2 & (T_{wo} \ge T_{s2}) \end{cases} \tag{1b}$$

where ρ_1 and ρ_2 are the reflectivity of OVW below the lower transition temperature T_{s1} and over the upper transition temperature T_{s2}, respectively. The difference between T_{s1} and T_{s2} is defined as temperature zone ΔT_s for optic-variation, the typical value of which is prescribed at 3 °C.

The heat flux Q can also be expressed as:

$$Q = \frac{T_{wo} - T_{ai}}{R} \tag{2a}$$

where R represents the global thermal resistance between T_{wo} and T_{ai}, and is determined by:

$$R = R_w + R_i \tag{2b}$$

where R_w refers to the conductive thermal resistance of OVW and insulation layer, and is expressed as:

$$R_w = \sum_j \left(\frac{\delta_j}{\lambda_j}\right) \tag{2c}$$

where δ_j and λ_j refers to the thickness and thermal conductivity of the layer with counting number j. R_i refers to the thermal resistance of indoor comprehensive heat transfer, and is expressed as:

$$R_i = \frac{1}{h_i} \tag{2d}$$

Combining Eqs. (1) and (2), the heat flux Q is determined by:

$$Q = \frac{(1-\rho)\cdot I - h_o\cdot(T_{ai} - T_{ao})}{1 + R\cdot h_o} \tag{3a}$$

and

$$\rho = \begin{cases} \rho_1 & (I \le I_1) \\ \rho_1 + \dfrac{(T_{ai} - T_{s1}) + R\cdot(h_o\cdot(T_{ao} - T_{s1}) + (1-\rho_1)\cdot I)}{(T_{s2} - T_{s1}) + R\cdot(h_o\cdot(T_{s2} - T_{s1}) + (\rho_2 - \rho_1)\cdot I)}\cdot(\rho_2 - \rho_1) & (I_1 \le I \le I_2) \\ \rho_2 & (I \ge I_2) \end{cases} \tag{3b}$$

where

$$I_1 = \left(\frac{1}{1-\rho_1}\right)\cdot\left(\frac{T_{s1} - T_{ai}}{R} + h_o\cdot(T_{s1} - T_{ao})\right) \tag{3c}$$

and

$$I_2 = \left(\frac{1}{1-\rho_2}\right)\cdot\left(\frac{T_{s2} - T_{ai}}{R} + h_o\cdot(T_{s2} - T_{ao})\right) \tag{3d}$$

4. Results and discussion

4.1. Ambient conditions

The profiles of ambient temperature and solar irradiance on a horizontal as well as on a vertical surface (facing south) in Shanghai, located in the East of China, are shown in Fig. 3. The minimum and maximum reflectivity, i.e. ρ_1 and ρ_2 are assigned as their theoretical values 0.1 and 0.9, respectively.

4.2. Variation of HVAC load

When T_{s1} and T_{s2} are designated as 23.5 °C and 26.5 °C, respectively, the variation of HVAC load on horizontal and vertical surfaces with ambient temperature T_{ao}, solar irradiance rate I_H or I_V as well as time t is depicted in Figs. 4–6. The indoor air temperature T_{ai} is prescribed as 25 °C.

Since positive Q corresponds to the cooling load and negative Q to the heating load, it is concluded from Fig. 4 that comparing with OFW (Optic-Fixed Wall), either high or low reflectivity as well as either horizontal or vertical, HVAC load is always reduced, thanks to OVW. Comparing with OFW with low reflectivity, the cooling load of OVW is smaller. On the contrary, the heating load of OVW is smaller, comparing with OFW with high reflectivity. Both two cases support the energy saving potential of OVW in buildings.

As found in Fig. 5, HVAC load with OVW, i.e. Q_H or Q_V is more discrete than OFW with high reflectivity, i.e. Q_{HH} or Q_{VH}, but less discrete than OFW with small reflectivity, i.e. Q_{HL} or Q_{VL}, when the ambient temperature T_{ao} is prescribed. In the case of high T_{ao}, the discretion of HVAC load with OVW is the same as OFW with high reflectivity. Meanwhile, in the case of low T_{ao}, the discretion of HVAC load with OVW offers smaller heating load than OFW with high reflectivity. Since the less sensitive to the solar irradiance, the more stable operation of HVAC system, it is concluded that OVW is favorable for the stable operation of HVAC system at cooling mode and is favorable for the reduction of HVAC load at heating mode.

It is also found that OVW demands only cooling load at high ambient temperature region and only heating load at low ambient temperature region, which is similar to the case of OFW with high reflectivity. However, in the case of OFW with small reflectivity, heating and cooling demands could shift during a day in the wide range of ambient temperature. Therefore, OVW is also favorable for

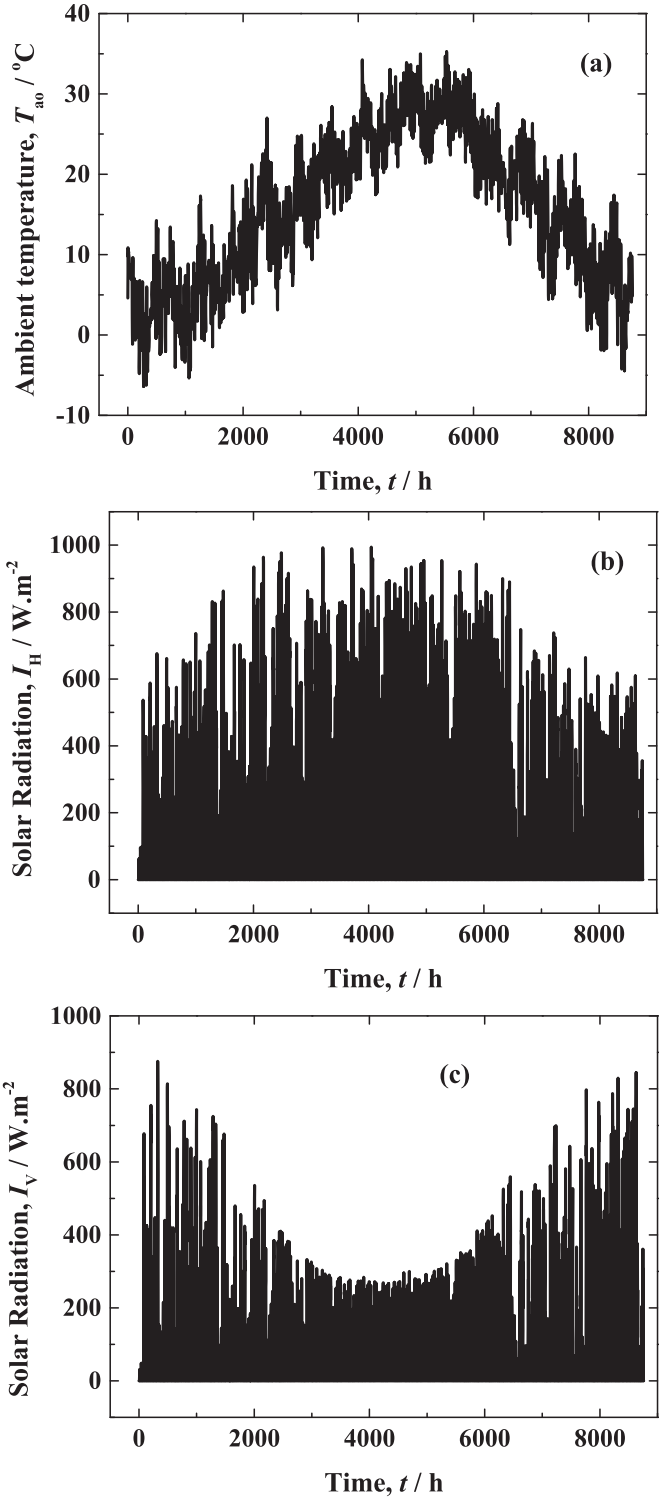

Fig. 3. Profile of air temperature and solar irradiance in Shanghai. (a) Air temperature; (b) Solar irradiance on horizontal surface and (c) Solar irradiance on vertical surface.

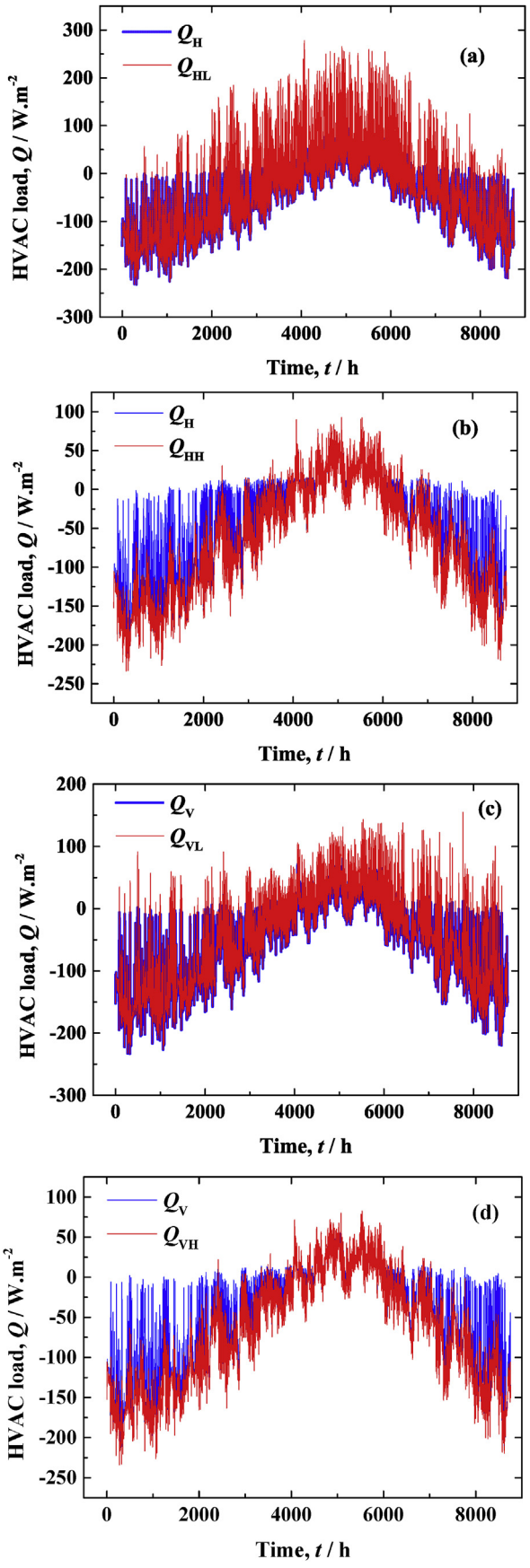

Fig. 4. Variation of HVAC load with time.

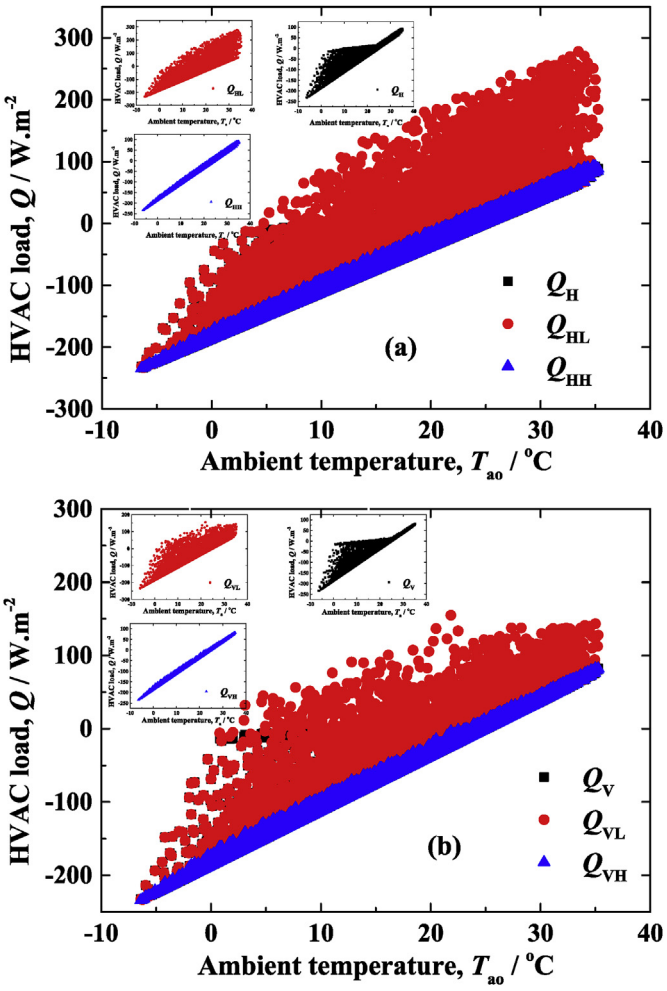

Fig. 5. Variation of HVAC load with ambient temperature. (a) Horizontal surface and (b) Vertical surface.

the control strategy of HVAC system operation with the criteria of ambient temperature T_{ao}.

The variation of HVAC load with solar radiation rate is shown in Fig. 6. Different from the discretion distribution of HVAC load at prescribed ambient temperature, comparing with OFW, OVW offers the least discretion at prescribed solar irradiance.

Comparing Figs. 5 and 6, it is found that comparing with solar radiation rate, the ambient temperature has more significant influence on the difference of HVAC load on horizontal and vertical surfaces. The difference between Fig. 6a and b is more obvious than that between Fig. 5a and b.

4.3. HVAC load in the whole year

As shown in Fig. 7, in the case of OFW, low reflectivity is favorable for the reduction of heating load, while high reflectivity is favorable for the reduction of cooling load. On the contrary, in the case of OVW, the cooling load and the heating load are simultaneously reduced. It is found that the heating load of OVW is close to that of OFW with low reflectivity, and the cooling load of OVW is close to that of OFW with high reflectivity. Therefore, OVW is favorable for the reduction of HVAC load, comparing with OFW with high or low reflectivity.

The comparison of HVAC load is also listed in Table 1. It should be mentioned that the heating load E_H of OVW is actually slightly

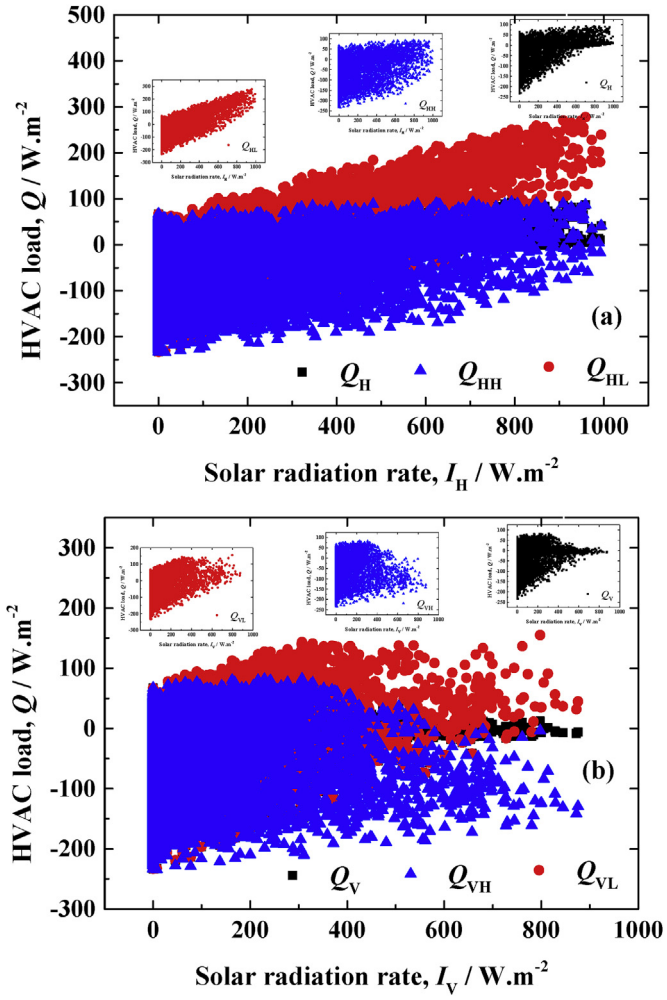

Fig. 6. Variation of HVAC load with solar irradiance. (a) Horizontal surface and (b) Vertical surface.

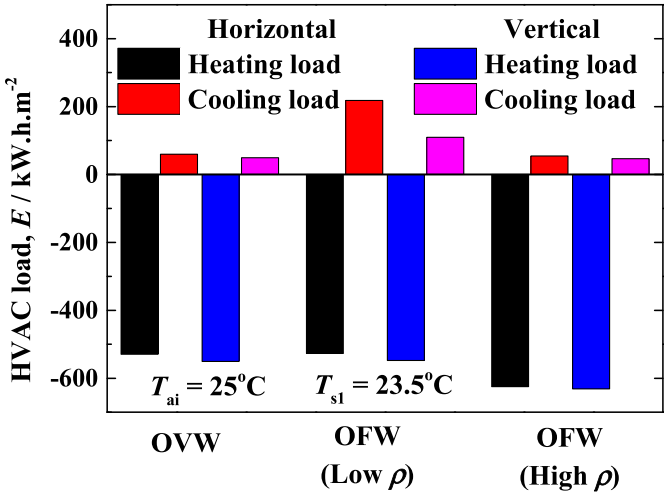

Fig. 7. HVAC load in the whole year.

larger than OFW with small reflectivity, on both the horizontal and the vertical surfaces, i.e. 2.7–2.8 kWh·m^{-2} (0.5%). However, comparing with the significant reduction of the cooling load E_C, i.e. 158.4–60.2 kWh·m^{-2} (266.2–121.6%), it is proper to announce that OVW is favorable for the reduction of HVAC load. Similar condition is also found in the case of comparison between OVW and OFW with high reflectivity, where the cooling load E_C is increased by 3.1–5.2 kWh·m^{-2} (6.3–8.7%) and the heating load E_H is decreased by 80.6–95.2 kWh·m^{-2} (14.6–18.0%), with the adoption of OVW.

4.3.1. Effects of onset temperature of OVW

The effects of onset temperature T_{s1} of OVW on the HVAC load are depicted in Fig. 8. It is found that HVAC load has similar variation trends on the horizontal and vertical wall. The cooling load is always larger on horizontal surface, while the heating load is larger on vertical surface. This is due to the less intensive solar radiation on vertical surface, as shown in Fig. 3.

Threshold temperature occurs in the profile of cooling and heating load. It is concluded as 25 °C and 22 °C for heating load E_H and cooling load E_C, respectively. When T_{s1} is lower than 22 °C, the cooling load E_C is independent of T_{s1}. The heating load E_H is independent of T_{s1}, when T_{s1} is larger than 25 °C.

Transition temperature is also found in the profile of HVAC load, which is concluded as 23.5 °C for both cooling and heating load. When T_{s1} is between 22 °C and 23.5 °C, E_C increases slightly with T_{s1}. When T_{s1} is higher than 23.5 °C, E_C increases sharply with T_{s1}. On the contrary, E_H decreases slightly with T_{s1}, when T_{s1} is ranging from 25 °C to 23.5 °C, while E_H decreases sharply with T_{s1}, when T_{s1} is lower than 23.5 °C.

Therefore, it is concluded that the optimal onset temperature T_{s1} of OVW is 23.5 °C, corresponding to half the temperature zone ΔT_s lower than the stable air temperature inside T_{ai}.

4.3.2. Effects of temperature zone of optic-variation

The variation of HVAC load reduction potential with the temperature zone ΔT_s of optic-variation is depicted in Fig. 9. The air temperature inside is prescribed at 25 °C. The onset temperature T_{s1} is designated half the temperature zone lower than the air temperature inside.

It is shown from Fig. 9 that the performance of OVW on the reduction of HVAC load decreases with the temperature zone of optic-variation. Therefore, it is suggested to develop more sensitive color-transformation, responding to the temperature variation, to narrow the temperature zone of optic-variation and correspondingly to reduce the HVAC load.

4.3.3. Effects of air temperature inside

The effects of indoor air temperature on the reduction of HVAC load are depicted in Fig. 10. It is concluded that with the increase of T_{ai}, OVW offers smaller absolute reduction of cooling load, comparing with OFW with low ρ and larger absolute reduction of heating load, comparing with OFW with high ρ. This implies that OVW offers better performance than OFW with low reflectivity, when the indoor air temperature is prescribed at low value; OVW offers better performance than OFW with high reflectivity, when the air temperature inside is prescribed at high value, as far as the absolute reduction of HVAC load is taken into consideration.

When the relative reduction of HVAC load is concerned, OVW shows stronger benefits on the reduction of cooling load, in the case of high air temperature inside, as compared with OFW with low reflectivity. However, comparing with high reflective OFW, OVW offers highest reduction of heating load at 15 °C of air temperature inside, on horizontal surface, and at 10 °C of air temperature inside, on vertical surface.

4.3.4. Effects of conductive thermal resistance

The variation of HVAC load reduction with the conductive thermal resistance of OVW is depicted in Fig. 11. The air temperature inside is designated as 25 °C. The temperature zone of OVW is

Table 1
Comparison of HVAC load in the whole year.

	Horizontal surface			Vertical surface		
	OVW	OFW		OVW	OFW	
		Low reflectivity	High reflectivity		Low reflectivity	High reflectivity
Heating load, E_H/kWh·m^{-2}	−529.4	−526.7	−624.6	−550.6	−547.8	−631.2
Absolute difference[a,b]/kWh·m^{-2}		2.7	−95.2		2.8	−80.6
Relative difference[a,c]/%		−0.5	18.0		−0.5	14.6
Cooling load, E_C/kWh·m^{-2}	59.5	217.9	54.3	49.5	109.7	46.4
Absolute difference[a,b]/kWh·m^{-2}		158.4	−5.2		60.2	−3.1
Relative difference[a,c]/%		266.2	−8.7		121.6	−6.3

Note.
[a] Comparison takes the HVAC load in the corresponding case of OVW as the basis.
[b] Positive value of absolute difference refers to larger cooling load or smaller heating load. Vice Verse.
[c] Positive value of relative difference refers to larger cooling load or larger heating load. Vice Verse.

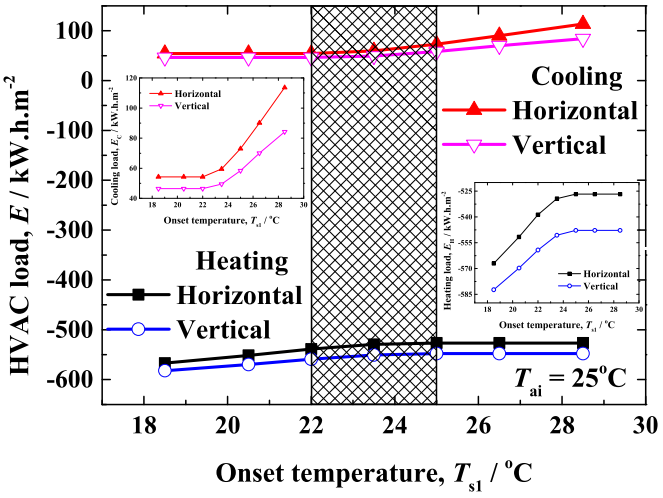

Fig. 8. Variation of HVAC load with onset temperature of OVW.

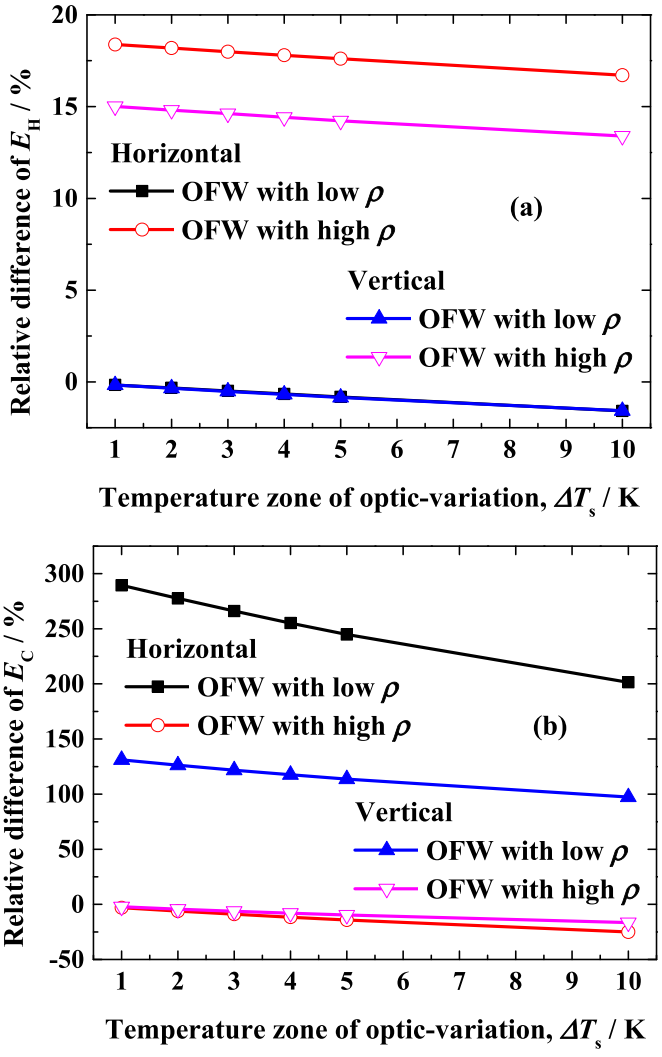

Fig. 9. Variation of HVAC load reduction with temperature zone of optic-variation. (a) Relative difference of E_H and (b) Relative difference of E_C.

prescribed as 3 °C. The corresponding results of HVAC load with OVW are taken as the basis for the estimation of absolute and relative difference.

It is concluded from Fig. 11 that the relative difference of heating and cooling load is almost independent of the conductive thermal resistance R_w. In the case of OFW and the absolute difference of heating and cooling load is slightly influenced by R_w, in the case of OFW with low and high reflectivity, respectively. Comparing with OFW with low reflectivity, the advantage of absolute reduction of cooling load decreases with the conductive thermal resistance. Similarly, comparing with OFW with high reflectivity, the advantage of absolute reduction of heating load decreases with the conductive thermal resistance.

Therefore, it is implied that with the adoption of OVW, the necessary thickness of thermal insulation layer, which is related to the conductive thermal resistance R_w, can be reduced. Moreover, even in the case of buildings with thick insulation layer, the adoption of OVW still offers obvious relative reduction of HVAC load, comparing with OFW.

5. Conclusion

The potential of energy saving with OVW for stable air temperature control in buildings by reducing the HVAC load was theoretically investigated in this paper. The effects of properties of OVW as well as the arbitrary prescribed air temperature inside on the reduction of HVAC load were discussed. The results offer new choices for green-building design and conclusions are made as follows:

(1) With the adoption of OVW, the HVAC load, including heating and cooling load, could be simultaneously reduced. Comparing with OFW with low reflectivity, the cooling load

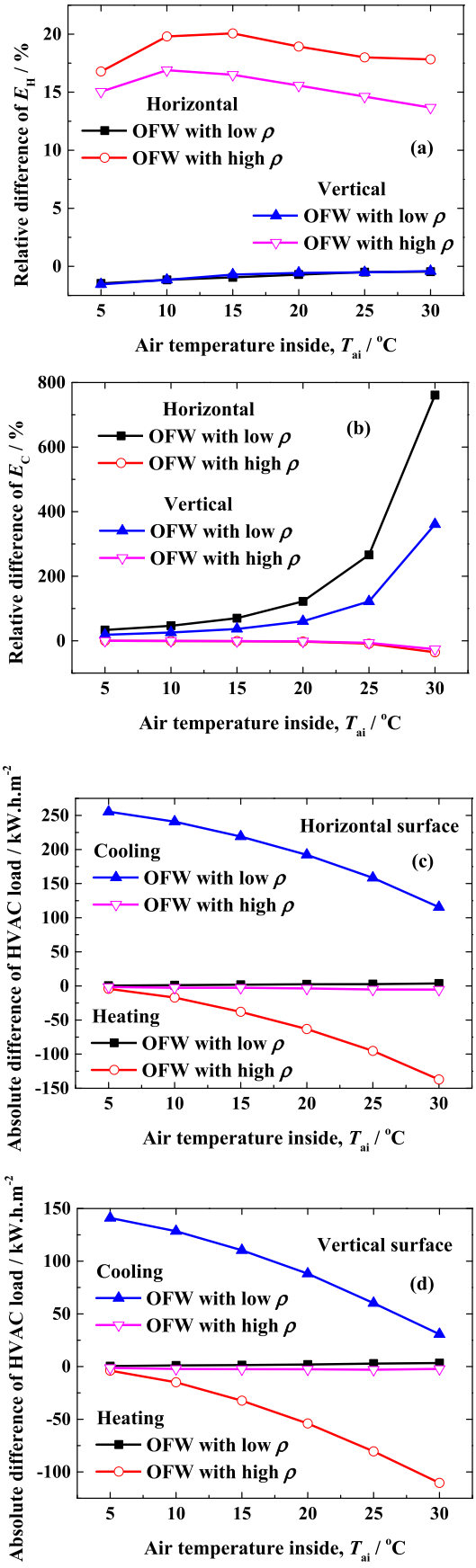

Fig. 10. Effects of air temperature inside on the reduction of HVAC load. (a) Relative difference of E_H; (b) Relative difference of E_C; (c) Absolute difference of HVAC load and (d) Absolute difference of HVAC load. Note: Corresponding results of OVW are taken as the basis of comparison. The onset temperature of OVW is designated as half the temperature zone lower than the air temperature inside.

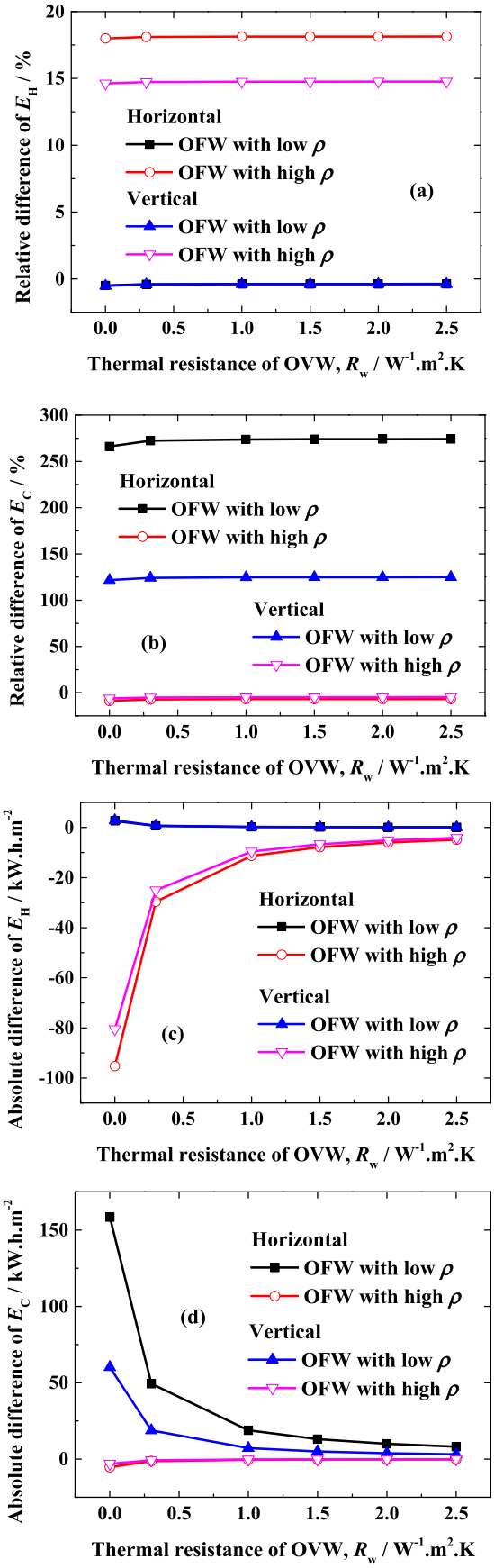

Fig. 11. Effects of conductive thermal resistance of OVW on HVAC load reduction. (a) Relative difference of E_H; (b) Relative difference of E_C; (c) Absolute difference of E_H and (d) Absolute difference of E_C.

is reduced. Comparing with OFW with high reflectivity, the heating load is reduced.

(2) The optimum onset temperature of OVW is half the temperature zone of optic-variation lower than the air temperature inside. When the onset temperature of OVW is higher or lower than the optimum value, the cooling or heating load would increase sharply, respectively.

(3) Narrow temperature zone of optic-variation is favorable for the reduction of HVAC. With the increase of temperature zone, the performance of OVW on the reduction of both heating and cooling load is weaker.

(4) The relative difference between OVW and OFW is independent of the conductive thermal resistance, which corresponds to the thickness of insulation layer. With weaker insulation, the absolute reduction of HVAC load with the adoption of OVW is more significant.

Our future works include the performance improvement of the OVW itself as well its application in urban heating and cooling reduction. In particular, the adaptability of the OVW for emergency cooling during heatwaves [35] will be evaluated by dynamic building energy simulation.

Acknowledgments

The present work is supported by the National Natural Science Foundation of China (No. 51306023), the French Ministry of Europe and Foreign Affairs (MEAE), through the PHC Xu Guangqi program (No: 41269UL, 2018) and the Jeunes Talents France Chine program (No: 925116B, 2018). The authors would like to acknowledge the support from Advanced Catalysis and Green Manufacturing Collaborative Innovation Center of Jiangsu.

Nomenclature

E	HVAC load in the whole year, $kWh \cdot m^{-2}$
h	convective heat transfer rate, $W \cdot m^{-2} \cdot K^{-1}$
I	solar irradiance, $W \cdot m^{-2}$
Q	heat flux, W
R	thermal resistance, $W^{-1} \cdot m^2 \cdot K$
t	time, h
T	temperature, °C

Greek symbol

δ	thickness of layer, m
Δ	difference
λ	thermal conductivity, $W \cdot m^{-1} \cdot K^{-1}$
ρ	reflectivity

Subscripts

1	lower set value
2	upper set value
ai	air inside
ao	ambient air
b	background
C	cooling
ci	coefficient inside
co	coefficient ambient
H	heating; horizontal surface with OVW
HH	horizontal surface with high reflectivity
HL	horizontal surface with low reflectivity
i	inside comprehensive coefficient
j	counting number
o	ambient comprehensive coefficient
r	reflective
s1	onset value of optic-variation
s2	offset value of optic-variation
V	vertical surface with OVW
VH	vertical surface with high reflectivity
VL	vertical surface with low reflectivity
w	wall
wo	outside of wall

Conflicts of interest

None declared.

References

[1] China Building Energy Use. Building Energy Research Center of Tsinghua University. China Architecture & Building Press; 2017. p. 22. ISBN 978-7-112-21714-4(31512).
[2] Kabeel AE, Abdelgaied Mohamed. Solar energy assisted desiccant air conditioning system with PCM as a thermal storage medium. Renew Energy 2018;122:632–42.
[3] Kabanshi Alan, Ameen Arman, Hayati Abolfazi, Yang Bin. Cooling energy simulation and analysis of an intermittent ventilation strategy under different climates. Energy 2018;156:84–94.
[4] Saghafifar Mohammad, Gadalla Mohamed. Performance assessment of integrated PV/T and solid desiccant air-conditioning systems for cooling buildings using Maisotsenko cooling cycle. Sol Energy 2016;127:79–95.
[5] Fong KF, Lee CK, Lin Z. Investigation on effect of indoor air distribution strategy on solar air-conditioning systems. Renew Energy 2019;131:413–21.
[6] Zhang Dongliang, Zhang Xu, Cai Ning. Study on energy saving possibility of digital variable multiple air conditioning system in three office buildings in Shanghai. Energy Build 2014;75:23–8.
[7] Mao Ning, Jingyu Hao, Cui Borui, Li Yuxing, Deng Shiming. Energy performance of a bedroom task/ambient air conditioning (TAC) system applied in different climate zones of China. Energy 2018;159:724–36.
[8] Lizana Jesus, Serrano-Jimenez Antonio, Ortiz Carlos, Becerra Jose A, Chacartegui Ricardo. Energy assessment method towards low-carbon energy schools. Energy 2018;159:310–26.
[9] Uysal Murat Pasa, Sogut M Ziya. An integrated research for architecture-based energy management in sustainable airports. Energy 2017;140:1387–97.
[10] Sum Wei, Ji Jie, Luo Chenglong, He Wei. Performance of PV-Trombe wall in winter correlated with south facade design. Appl Energy 2011;88:224–31.
[11] Rabani Mehran, Kalantar Vali, Dehghan Ali A, Faghih Ahmadreza K. Experimental study of the heating performance of a Trombe wall with a new design. Sol Energy 2015;118:359–74.
[12] Barzin Reza, Chen John JJ, Young Brent R, Farid Mahammed M. Application of PCM energy storage in combination with night ventilation for space cooling. Appl Energy 2015;158:412–21.
[13] Kazanci Ongun B, Skrupskelis Martynas, Sevela Pvel, Pavlov Georgi K, Olesen Bjarne W. Sustainable heating, cooling and ventilation of a plus-energy house via photovoltaic/thermal panels. Energy Build 2014;83:122–9.
[14] Aissani A, Chateauneuf A, Fontaine JP, Audebert Ph. Quantification of workmanship insulation defects and their impact on the thermal performance of building facades. Appl Energy 2016;165:272–84.
[15] Mintorogo Danny Santoso, Widigdo Wanda K, Juniwati Anik. Application of coconut fibres as outer eco-insulation to control solar heat radiation on horizontal concrete slab rooftop. Procedia Engineering 2015;125:765–72.
[16] Zeng Ruolang, Wang Xin, Di Hongfa, Jiang Feng, Zhang Yinping. New concepts and approach for developing energy efficient buildings: ideal specific heat for building internal thermal mass. Energy Build 2011;43:1081–90.
[17] Hu Mingke, Zhao Bin, Ao Xianze, Su Yuehong, Pei Gang. Parametric analysis and annual performance evaluation of an air-based integrated solar heating and radiative cooling collector. Energy 2018;165:811–24.
[18] Zhao BY, Li Y, Wang RZ, Zhao ZG, Taylor RA. A universal method for performance evaluation of solar photo-voltaic air-conditioner. Sol Energy 2018;172:58–68.
[19] Kazanci Ongun B, Skrupskelis Martynas, Sevela Pvel, Pavlov Georgi K, Olesen Bjarne W. Sustainable heating, cooling and ventilation of a plus-energy house via photovoltaic/thermal panels. Energy Build 2014;83:122–9.
[20] Zhang Weilong, Lu Lin, Peng Jinqing. Evaluation of potential benefits of solar photo-voltaic shadings in Hong Kong. Energy 2017;137:1152–8.
[21] Prieto Alejandro, Ulrich Knaack, Auer Thomas, Klein Tillmann. Solar cool-facades : framework for the integration of solar cooling technologies in the building envelope. Energy 2017;137:353–68.
[22] Bansal NK, Garg SN, Kothari S. Effect of exterior surface colour on the thermal performance of buildings. Build Environ 1992;27(1):31–7.
[23] Lei Jiawei, Kumarasammy Karthikeyan, Zingre Kishor T, Yang Jinglei, Wan Man Pun, Yang En-Hua. Cool colored coating and phase change materials as complementary cooling strategies for building cooling load reduction in tropics. Appl Energy 2017;190:57–63.
[24] Guo W, Qiao X, Huang Y, Fang M, Han X. Study on energy saving effect of heat-

reflective insulation coating on envelopes in the hot summer and cold winter zone. Energy Build 2012;50:196–203.
[25] Antonaia Alessandro, Ascione Fabrizio, Castaldo Anna, D'Angelo Antonio, De Masi Rosa Francesca, Ferrara Manuela, Vanoli Guiseppe Peter, Vitiello Guiseppe. Cool materials for reducing summer energy consumptions in Mediterranean climate: in-lab experiments and numerical analysis of a new coating based on acrylic paint. Appl Therm Eng 2016;102:91–107.
[26] Leo Samuel DG, Shiva Nagendra SM, Maiya MP. Passive alternatives to mechanical air conditioning of building: a review. Build Environ 2013;66:54–64.
[27] Long Linshuang, Ye Hong, Liu Minghou. A new insight into opaque envelopes in a passive solar house: properties and roles. Appl Energy 2016;183:685–99.
[28] Lee Sau Wai, Lim Chin Haw, Salleh Elias Ilias Bin. Reflective thermal insulation systems in buildings: a review on radiant barrier and reflective insulation. Renew Sustain Energy Rev 2016;65:643–61.
[29] Cheng V, Ng E, Givoni B. Effect of envelope colour and thermal mass on indoor temperatures in hot humid climate. Sol Energy 2005;78(4):528–34.
[30] Wang C, Zhu Y, Qu J, Hu HD. Automatic air temperature control in a container with an Optic-Variable Wall. Appl Energy 2018;224:671–81.
[31] Goldstein Eli A, Raman Aaswath P, Fan Shanhui. Sub-ambient non-evaporative fluid cooling with the sky. Nature Energy 2017. https://doi.org/10.1038/nenergy.2017.143.
[32] Zhao DL, Aili A, Zhai Y, Tan G, Yin XB, Yang RG. Subambient cooling of water: toward real-world applications of daytime radiative cooling. Joule 2018. https://doi.org/10.1016/j.joule.2018.10.006.
[33] Zhu Jiayin, Chen Bin. Experimental study on thermal response of passive solar house with color changed. Renew Energy 2015;73:55–61.
[34] Zhang Y, Long E, Li Y. Solar radiation reflective coating material on building envelopes: heat transfer analysis and cooling energy saving. Energy Explor Exploit 2017;35:748–66.
[35] Guo Xiaofeng, Martin Hendel. Urban water networks as an alternative source for district heating and emergency heat-wave cooling. Energy 2018;145:79–87. https://doi.org/10.1016/j.energy.2017.12.108.